Correlation of Vibratory Hub Loads for a Sikorsky Full-Scale Bearingless Main Rotor

James M. Wang
Dynamicist

Sikorsky Aircraft Division
United Technologies Corporation
Stratford, CT

Johannes M. van Aken
Research Engineer

Sterling Software
NASA Ames Research Center
Moffett Field, CA

ABSTRACT

A comparison of measured and predicted vibratory hub loads for a bearingless main rotor (BMR) is presented. The measured data are from a full-scale wind tunnel test of the Sikorsky 5-bladed proof-of-concept BMR that is sized for the Sikorsky S-76 helicopter. Three rotorcraft analyses are used for the predictions. They are: the Sikorsky KTRAN and RDYNE analyses, and the Sikorsky modified version of the UMARC analysis.

INTRODUCTION

Jet-smooth ride has been an elusive goal for helicopters. One of the keys lies in reducing the vibratory hub loads. However, accurate measurement and prediction of rotor vibratory loads remain a challenge for rotorcraft researchers. For a bearingless rotor, which has multiple load paths and complex structural and kinematic couplings, the accurate prediction of loads becomes a greater challenge. The objective of this paper is to present results from a recent correlation study of vibratory hub loads for a full-scale bearingless main rotor.

The hub load data used were obtained from an extensive wind tunnel test of the Sikorsky proof-of-concept 5-bladed full-scale bearingless main rotor conducted in 1992 at the NASA Ames 40- by 80- Foot Wind Tunnel of the National Full-Scale Aerodynamic Complex (Ref. 1). This BMR (Fig. 1) is a 44 ft diameter main rotor sized for the Sikorsky S-76 helicopter. The wind tunnel test included flight conditions from 0 to 200 knots, and thrust levels from -4,000 to 18,000 pounds. Parametric sweeps were conducted to systematically examine the effects of rotor speed, forward flight speed, thrust level, cyclic pitch, and shaft tilt on BMR response and loads. Hub loads were measured using several techniques: accelerometers on the rotating hub, strain gauges on the rotor shaft, and a five-component balance in the fixed reference frame. This test has provided a rare opportunity to validate the state-of-the-art in BMR load prediction methodology.

The paper first describes the Rotor Test Apparatus (RTA), the Steady/Dynamic Rotor Balance, and the RTA rotor control system. Subsequently, the shaft bending gauge installation, the dynamic calibration procedures for the balance, the non-rotating pushrods, and the shaft bending gauges are described. Experimental 5/rev hub loads from the balance and the shaft bending gauges are shown for an airspeed sweep at constant thrust and prescribed hub moments. These experimental data are compared with theoretical predictions from KTRAN, RDYNE, and UMARC/S. These three codes have been used very successfully at Sikorsky for predicting the blade frequencies, blade response, blade bending moments, and stability of this BMR (Refs. 2, 3 and 4).

Presented at the 50th Annual Forum of the American Helicopter Society, Washington D.C., May 11-13, 1994.

Description of Experiment

Traditionally, it has been difficult to accurately measure vibratory hub loads (Ref. 5). In order to get a reliable estimation, three hub load measuring methods were used in this test. Figure 2 shows the location of the hub accelerometers, the shaft bending gauges, and the balance. The shaft bending gauges are mounted on the rotating shaft, which sits inside the stove pipe. Experimental data were obtained over a wide range of test conditions and included the following parametric sweeps:

- Hover collective pitch sweep, θ_{75} from 0.7 deg to 11.7 deg, in 1 deg increments.
- Hover rotor speed sweep from 283 to 346 rpm.
- Forward flight speed sweep at 10,500 lb from 0 to 200 knots.
- Forward flight speed sweep at 14,000 lb from 0 to 160 knots.
- Forward flight speed sweep at 16,000 lb from 0 to 140 knots.
- Thrust sweep at 80 knots from -4,000 to 15,500 lb.
- Thrust sweep at 120 knots from -1,835 to 15,700 lb.
- Shaft angle sweep at 80 knots from +5 deg nose up to -10 deg nose down.
- Rotor speed sweep at 40, 60, 120 and 160 knots, from 255 to 330 rpm.
- Rotor head moment sweep from -15,000 to +15,000 ft-lb in pitch and roll.

Rotor Test Apparatus

The rotor was mounted on NASA Ames' Rotor Test Apparatus (RTA). The RTA is a special-purpose drive and support system for operating helicopter rotors in the 40- by 80- Foot or the 80- by 120-Foot Wind Tunnels. The RTA houses two 1500 horsepower electric drive motors, the hydraulic servo-actuators of the primary control-system, and a dynamic control system capable of introducing dynamic perturbations to the swashplate at frequencies up to 40 Hz. Recent modifications to the RTA include the addition of a five-component balance to measure steady and vibratory rotor loads at up to 22,000 lb thrust. The balance natural frequencies are all above 60 Hz. An instrumented flex-coupling measures rotor torque and residual thrust. The RTA is mounted on three vertical struts. The rotor plane is approximately 22 feet above the tunnel floor. The RTA can be tilted forward or aft to change the rotor shaft angle.

Steady/Dynamic Rotor Balance

The five-component Steady/Dynamic Rotor Balance (S/DRB) is located between the RTA transmission and upper housing. A brief description of the balance is provided here, a detailed discussion is in Ref. 6.

The balance consists of two rings with a 28-in inner diameter and a 32-in outer diameter, which are connected to each other by four rectangular, instrumented flexures. The centers of the four flexures are located on a 30-in diameter circle. The balance peak load capacities are: 22,000 lb of thrust, 4,400 lb of resultant shear force, and 57,800 ft-lb of resultant moment at the balance moment center. The maximum allowable resultant hub moment depends upon the hub height above the balance moment center. The balance shares a common centerline with the rotor shaft. The rotor shaft has an in-line flex-coupling, which is instrumented to measure rotor torque up to a maximum of 36,000 ft-lb and the residual shaft thrust up to a calibration limit of 200 lb. The vibratory load capabilities of the balance are: 5,500 lb of thrust, 1,100 lb of resultant shear force, and 8,920 ft-lb of resultant moment.

RTA Rotor Control System

The three primary hydraulic actuators provide static control of the swashplate. The three non-rotating pushrods, connecting the walking beams to the swashplate, are approximately parallel to the rotor shaft and are located on an approximately 0.7 foot radius circle at azimuth locations of 120, 210, and 300 degree with 0 degree azimuth pointing aft along the RTA longitudinal axis. The non-rotating pushrods are instrumented to measure the pushrod's axial force.

The rotor control system is installed onto the RTA upper housing, which in turn is installed onto the five component fixed frame rotor balance. The balance measurements represent the total rotor loading which is transferred down from the rotor to the balance through the primary load path (formed by the rotor shaft and upper housing), and through the secondary load path

(formed by the torque tube, rotating pushrods, swashplate, walking beam, and non-rotating pushrods). Figure 2 illustrates this redundant load path system. To obtain the hub loads it is therefore necessary to correct the measured balance loading for the load contributions from the secondary load path (i.e., the control loads).

Shaft Bending Gauges

A total of four shaft bending gauges were installed on the RTA rotor shaft. These gauges are located at two different shaft heights and in two perpendicular planes, which go through the shaft centerline (Fig. 2). This combination allows the determination of the fixed frame drag force Fx, side force Fy, roll moment Mx and pitch moment My.

Dynamic Calibration

Prior to tunnel entry the five-component balance, flex-coupling, non-rotating pushrods, and shaft bending gauges were all statically calibrated. An extensive static calibration was performed with the balance installed inside the RTA. The resulting static calibration matrix corrects for first and second order single load interactions and for first order combined load interactions. The balance static data reduction program uses an iterative method to account for the fact that the balance static calibration was performed with only one or two balance gauges loaded, whereas in the wind tunnel test all balance gauges were loaded simultaneously.

The non-rotating pushrods were calibrated in a tension/compression calibration machine. The shaft bending moment gauges were statically calibrated in the 40- by 80- Foot Wind Tunnel by fixing a 200 inch long steel beam horizontally on top of the rotor shaft. Weight baskets were hung from each end of the steel beam and a hub moment was generated by transferring weights between these weight baskets. The steel beam was rotated 90 degree with respect to the shaft to calibrate all four shaft bending gauges. Only the static sensitivities were determined; no static corrections were made for shaft bending gauge interactions.

An extensive shake test was performed on the RTA in the 40- by 80- Foot Wind Tunnel to obtain the balance/stand frequency response functions (T_1) which represent the dynamics of the RTA installation. These FRF data were obtained with the RTA at zero degree angle of attack. A shake test was also performed on the non-rotating pushrods to get a frequency response function (T_2), which represents the dynamics of the pushrod load path. The dynamic calibration of the balance is extensively discussed in Ref. 6 and that effort is being extended here to include the dynamic calibration of the pushrods and the shaft gauges.

The dynamics of the RTA stand is eliminated by multiplying the measured balance data by the inverse of the RTA stand transfer function (T_1). The loads from the pushrods must be subtracted to obtain the true loads coming from the rotor shaft. The corrected balance loads become:

$$F = [T_1]^{-1} \cdot S - [T_2] \cdot P$$

5x1	5x5	5x1		5x3	3x1
Corrected balance loads	load /mv	Measured balance signal (mv)		load /load	Stationary pushrod load

The corrected balance loads are then transferred to the hub to obtain the rotor thrust, hub shear forces, and hub moments.

Shake Test Procedure

For the shake test, the rotor hub was replaced by special shake test hardware, which allowed for vertical hub load application at the shaft center and at a radial moment arm of 1 ft and for horizontal hub shear loading (Ref. 6). A hydraulic actuator was used to excite the model and the support system at the nominal hub height of 6.1 ft above the balance moment center. One end of the hydraulic actuator was attached to a 5-ft-long extension arm. The other end of the actuator was attached to the hub. The extension arm was attached to an 11,600 lb reaction mass hung from the gantry crane, as shown in Fig. 3. The actuator was aligned with respect to the extension arm, which was in turn aligned parallel to the shake direction. Fine alignment of the load direction was obtained through guy wires between the reaction mass and the tunnel walls. The guy wires also restrained swinging of the reaction mass during actuator excitation. A load cell

located between the hydraulic actuator and the hub measured the applied force.

A random excitation from 0-64 Hz at input force levels of up to +/-600 lb rms was applied in the balance and shaft bending gauge shake tests. A 16-channel GenRad 2515 Computer-Aided Test System was used to acquire and store the FRFs of the balance forces and moments and shaft bending moments with respect to the input force load cell. A 512-point Fast Fourier Transform (FFT) was performed to obtain the FRF data. The spectral line resolution is 0.125 Hz. The FRF data were then transferred to a VAX mainframe computer for further data processing.

For determining the dynamic calibration matrix for the balance, the shake test hardwares on top of the rotor shaft simulated the weight of the BMR hub, only. A total of five unique load sequences were applied: vertical loading at the shaft center (thrust loading), vertical loading at one foot forward of the shaft center (thrust and hub pitch moment loading) and at one foot to the left of the shaft center (thrust and hub roll moment loading), and hub horizontal loading in the RTA longitudinal plane (hub axial force loading) and in the RTA lateral plane (hub side force loading). The FRF data in terms of balance gauge output over balance gauge applied loading were obtained for each of the five balance gauges. Note, due to the offset between the balance moment center and the hub, a horizontal hub loading results in balance force and moment loading.

The shake test data analysis program calculates the complex 5-by-5 T_1 balance dynamic response matrix at each spectral line. Each element in this response matrix represents the FRF value of a balance gauge due to a single balance gauge loading. The complex response matrix is subsequently inverted to obtain the complex dynamic calibration matrix at each spectral line. This calibration matrix incorporates first order dynamic corrections for single load gauge interactions.

A shake test was also performed on the three non-rotating pushrods by applying a random excitation from 0-64 Hz at input levels of up to +/- 100 lb rms to each pushrod along its axis. To obtain access to the pushrods, it was necessary to remove the shake test hardware and acquire the FRFs at zero hub and zero blade mass. The FRFs of the balance forces and moments with respect to the input force load cell were acquired for each pushrod. The FRF data for the three non-rotating pushrods were subsequently combined into a 5-by-3 T_2 balance response to control system loading matrix at each spectral line.

For the dynamic calibration of the shaft bending moment gauges, the shake test hardware was configured to simulate the mass of the BMR hub and blades. Time constraint did not permit conducting another shake test without the blade mass. The shaft was aligned such that the shaft bending moment measurement planes were aligned with the RTA fuselage longitudinal and lateral planes. The RTA was at zero degree angle of attack. A random excitation from 0-64 Hz at input force levels of up to +/- 600 lb rms was applied at the nominal hub height to the non-rotating shaft in the longitudinal and lateral directions. The FRFs of the four shaft bending moment gauges were acquired with respect to the input force load cell. The upper and lower shaft gauges are located at 1.75 ft and 2.50 ft below the hub, respectively. The applied shaft bending moment equals the applied hub shear load times the hub-to-gauge distance.

The shake test data analysis program treats the upper and the lower shaft gauges as two independent two-component moment measurement devices. The lateral and longitudinal shake FRF data for each set of two gauges is used to determine a 2-by-2 dynamic response matrix at that particular shaft height. The inverse of the response matrix provides the complex dynamic shaft gauge calibration matrix. The matrix incorporates a first order dynamic correction for gauge interactions. This process is performed at each spectral line for both the upper and lower shaft bending moment gauge sets.

Wind Tunnel Data Reduction Procedures

For each test point, eight revolutions of data were collected at 64 samples per revolution. NASA's Rotor Data Reduction System (RDRS) program is used for off-line data reduction. The data are harmonically analyzed into the frequency domain and corrected for the analog filter settings and time skew. The balance and shaft bending data are then corrected at each harmonic for both

magnitude and phase using the dynamic calibration matrices.

The shake test FRFs are composed of a finite number of spectral lines with a spectral line resolution of 0.125 Hz. The RDRS program determines the FRF spectral lines (frequencies) nearest to an n/rev harmonic, and performs a linear interpolation on the elements of the balance and shaft gauge dynamic calibration matrices and of the dynamic balance/pushrod response matrix at the next higher and lower spectral line to determine the dynamic matrix at the n/rev harmonic. The shake test FRF data allow for dynamic corrections up to the 12/rev harmonic. The 1/rev frequency for this BMR is 5.25 Hz.

To determine the corrected hub loads from the balance measurements, the dynamically corrected balance data are first corrected for the loading coming through the redundant load path by subtracting the dynamic balance response from the redundant load path. The corrected balance loading is then transferred to the hub to obtain the rotor thrust, hub shear forces, and hub moments. The rotor thrust is then further corrected for the residual thrust measured by the shaft flex-coupling.

The dynamic calibration matrices for the shaft gauges were determined for a non-rotating shaft. Therefore, the rotating shaft bending moment harmonic data are first converted to non-rotating shaft moment harmonic data in the RTA fuselage longitudinal and lateral planes. These non-rotating moment data are multiplied with the dynamic calibration matrices for the upper and lower gauge sets. The resulting four dynamically corrected non-rotating shaft bending moments are subsequently transferred to the hub to provide the non-rotating hub shear forces and hub moments.

Any effect that shaft rotation might have on the response of the shaft bending moment gauges has been neglected here. The dynamic response seen by the shaft gauges is assumed to be due to the dynamic response of the RTA/stand and it is assumed that the dynamic corrections can be applied to the calculated moments in the non-rotating frame as obtained from the rotating shaft gauges. Reference 6 shows that the response of the balance to moments was slightly different for balance moments resulting from inplane hub forces versus out-of-plane hub forces. It is reasonable to expect that the shaft gauges, which are assumed here to measure the RTA/stand dynamic response, are also sensitive to the inplane versus out-of-plane moment generation. However, no shaft frequency response calibration data were acquired for out-of-plane moments.

Inplane hub loads are also obtained from the rotating acelerometers. The rotating frame accelerations are transformed to two orthogonal directions in the fixed frame. These accelerations are multiplied by the force/acceleration FRFs measured during the shake test to get the inplane hub loads.

Analytical Methodologies

The modeling of a bearingless rotor system is more involved than that of a hingeless, or articulated rotor system because of redundant load paths, elastomeric snubber/damper assemblies, and nonlinear structural couplings. Due to a lack of available test data and limited analytical tools, only limited analytical work has previously been done to correlate vibratory hub loads for bearingless rotors. The S-76 BMR data are invaluable for validating the different predictive methodologies.

Three separate analyses have been refined at Sikorsky to predict the dynamics of a BMR. The three analyses use different solution techniques. A comparison of the measured and predicted rotor stability and blade bending moments for this BMR is presented in Refs. 2 and 3, respectively. Reference 3 shows the analyses give a good prediction of blade loads for the S-76 BMR. As a continuation, the hub load data from the flight conditions of Ref. 3 are used for the correlations in this paper. A brief description of the three computer programs is given here.

KTRAN

KTRAN (Ref. 3) was developed at Sikorsky Aircraft for the prediction of rotor loads and response. The analysis includes coupled elastic flap, lag and torsion degrees of freedom. Fuselage dynamics are not included. The blade equations of motion are solved using the finite segment transfer matrix method. The bearingless rotor is

modeled as a multiple load path system with fifty discrete beam elements for the blade and flexbeam, and twenty beam elements for the torque tube (Fig. 4). Control system stiffness is modeled with a torsion spring connected between the ground and the torque tube. The snubber/damper is modeled as a spring and damper system linked between the torque tube and the flexbeam. The spring/damper model rotates with the torque tube. Blade element theory and airfoil table lookup are used for aerodynamic calculations. Variable rotor induced inflow is accounted for by geometric influence coefficients derived from the UTRC Freewake program (Ref. 7). The free wake enhances the prediction of higher harmonic aerodynamic forces. KTRAN can be trimmed to converge on prescribed rotor thrust and rotor moments, or to prescribed control settings. The hub loads are obtained by transforming the forces and moments at the root of the flexbeam into fixed frame. The advantage of the transfer matrix method is that the shear forces and moments at each element are part of the degrees of freedom, hence, there is no need to sum up the spanwise loads to find the loads at the flexbeam root.

RDYNE

RDYNE (Rotorcraft Dynamics Analysis, Ref. 4) is a comprehensive rotor trim/time history program developed at Sikorsky. It is a modal analysis, where the blade modes can be calculated internally, or imported from another analysis. For this paper, the modes used in RDYNE were imported from KTRAN. The blade response solution is obtained by a time-marching procedure. Quasi-steady blade element aerodynamic theory is used. Once the solution has converged, the generalized influence coefficients from the Freewake program (Ref. 7) are imported into RDYNE. The integrated time responses are post-processed to obtain the frequency content, rotor stability, and hub loads. The hub loads are obtained using a force summation method. The forces and moments along the blade, flexbeam, and torque tube are summed up to find the loads at the root of the flexbeam.

UMARC/S

UMARC/S (Refs. 2 and 3) is the Sikorsky version of the University of Maryland Advanced Rotorcraft Code (Ref. 8). The University of Maryland's UMARC analysis has been modified at Sikorsky to analyze the Comanche and S-76 BMR with a snubber/damper. UMARC is based on a finite element method in space and time. The hub motions are not included in the response calculations. The blade is assumed to be an elastic beam undergoing flatwise bending, chordwise bending, elastic twist and axial extension. This Bernoulli-Euler beam is allowed small strains and moderate deflections. For this BMR, five beam elements are used for modeling the blade, six for the flexbeam, and five for the torque tube. Each element has fifteen degrees of freedom (Refs. 3 and 8). The snubber/damper is modeled as a spring and damper system linked between the flexbeam and the torque tube. The spring/damper system rotates with the torque tube when blade pitch is changed. The aerodynamic modeling includes quasi-steady strip theory, the Leishman and Beddoes 2-D unsteady aerodynamic model for capturing the unsteady shed wake, and a Scully free wake to capture the 3-D trailed wake and higher harmonic forcing. The hub loads are obtained by the force summation method.

Results and Discussion

Experimental Results

Experimental data were obtained over a wide range of test conditions. Airspeed sweeps from 0 to 200 knots were performed at thrust levels ranging from -4,000 to 18,000 lb. Parametric sweeps were conducted to examine the effects of rotor speed, airspeed, thrust level, cyclic pitch, and shaft tilt on the BMR response and loads. The experimental data reported here are restricted to the 5/rev hub loads for an airspeed sweep from 40 to 150 knots at a thrust level of 14,000 lb. The wind tunnel trim conditions were set based upon pre-test Genhel (a Sikorsky nonlinear helicopter trim program) predictions for a helicopter in steady level flight. Figure 5 shows the wind tunnel trim conditions as measured by the balance. The fore/aft shaft tilt angle varied from $+1.0^{\circ}$ (aft) to -4.6° (forward). The nominal rotor speed was 315 rpm, which places the 5/rev harmonic at 26.25 Hz.

All hub forces and moments are with respect to the shaft axis system, with the origin located at the hub. Drag force is positive aft, and side force

is positive to the right when looking down onto the rotor disk. Roll moment is positive right side down and pitch moment is positive nose up. Their orientations are shown in Fig. 2. All the vibratory hub load data have been normalized by a constant: the same constant used for normalizing the blade bending moments in Ref. 3.

Figure 6 shows the normalized 5/rev hub load magnitude measured by the balance. The three lines represent hub loads (1) with static calibration for the balance, (2) with dynamic calibration for the balance, and (3) with dynamic calibration for the balance and the dynamic loads from the pushrods removed.

Figure 6 shows that including the dynamic balance corrections to account for the RTA/stand dynamics has a great influence on the 5/rev hub loads. Reducing the balance measurements with only the static calibration matrix results in significant overprediction of the 5/rev hub loads. The trends of the shear force measurements (Figs. 6a and 6b) as a function of forward velocity are consistent between the static and dynamic balance measurements. The dynamically corrected hub moments (Figs. 6c and 6d) show a different trend from the static calibration results, especially the roll moment; the dynamically corrected moments do not show the bucket type curve seen for the static balance measurements. Figure 6e shows the effect of dynamic balance corrections is small for the vertical 5/rev loads.

The non-rotating pushrods are approximately parallel to the rotor shaft, and as expected the dynamic pushrod corrections on horizontal hub shear forces are relatively small (Figs. 6a and 6b). However, in Figs. 6c and 6d, the pushrod load corrections substantially increase the hub moments at the low speeds. This illustrates the importance of correcting the hub load data for the loads through the secondary load path. Figure 6e shows the effect of the pushrod load correction on 5/rev vertical loads is also small (Fig. 6c).

Figure 7 shows the normalized 5/rev hub loads obtained from the shaft bending gauges. Data are shown with and without dynamic corrections for the RTA/stand dynamic response. The effect of dynamic corrections are most noticeable for the side force and roll moment.

Correlation of Experiment and Theory

Fig. 8 shows the predicted 5/rev pitch and roll moment from UMARC/S, with and without a free wake. Without a distorted free wake modeling, all three analyses predict almost zero 5/rev hub loads at low speed (40-60 knots).

Figure 9 presents the measured and predicted 5/rev hub loads at the 14,000 lb thrust condition as a function of forward velocity. The results from all three analyses include free wake modeling. KTRAN and RDYNE use the UTRC Freewake (Ref. 7), and UMARC/S uses the Scully free wake. The measured data are all corrected for the dynamic response of the RTA/stand. The hub load data obtained from the balance has been corrected for the loads through the secondary load path; i.e., the dynamic pushrod load corrections have been applied. Hub shear forces as obtained from the hub accelerometer data are also shown in Fig. 9a and 9b. However, they are not as accurate as those obtained from the balance and the shaft bending gauges.

Figure 9a shows the normalized 5/rev drag force. Good agreement is seen between the measurements from the balance and the shaft gauges. The accelerometer data over-predicts the drag force. The KTRAN predictions show excellent correlation with the shaft and balance data at most of the airspeeds, but fail to predict the increase in 5/rev drag load at 150 knots. UMARC/S over-predicts the drag loads at velocities below 100 knots, but show excellent agreement with data at higher airspeeds. RDYNE predictions are high for most of the speed range, although RDYNE does predict the increase at 150 knots. The difference in measured hub loads from the shaft gauges and from the balance could be partly due to the fact that a different mass was used in the two shake tests, from which the dynamic calibration matrices for the shaft gauges and for the balance were calculated.

Figure 9b shows the normalized 5/rev side force. The 5/rev side forces measured by the balance and accelerometer show similar trends, but the shaft bending gauges show higher loads above 80 knots. UMARC/S shows the the same bucket type curve as seen in the data. UMARC/S predicts the rise in 5/rev side force at 150 knots very well. RDYNE also captures the bucket type curve, but

does not predict the rise in vibratory loads at 40 knots. The magnitudes predicted by KTRAN are in agreement with the balance and accelerometer measurements, but KTRAN does not show the rise in loads at 40 knots and 150 knots.

Figure 9c presents the normalized 5/rev pitch moment comparison. Good agreement is seen between the measurements from the balance and the shaft gauges. UMARC/S over-predicts the 5/rev pitch moment at 40 and 60 knots, but does very well all other airspeeds. KTRAN predicts the 5/rev pitch moment extremely well. RDYNE does not predict the right trend or magnitude for the 5/rev pitch moment.

The normalized 5/rev roll moment comparison is shown in Fig. 9d. Excellent agreement is seen between the measurements from the balance and the shaft gauges at speed between 60 and 120 knots. But the shaft gauges show much larger roll moments at 40 knots and high speeds. All three analyses show the increase in 5/rev roll moment at 150 knots. The UMARC/S predictions match the balance data at 40 to 120 knots and then gives the same trend as the shaft bending data from 120 to 150 knots. KTRAN under-predicts the 5/rev roll moment at most airspeeds, but matches the shaft bending data at 120 to 150 knots very well. RDYNE shows similar trend as UMARC/S, except RDYNE under-predicts the loads between 40 and 80 knots.

Figure 9e shows the normalized 5/rev vertical hub loads. Experimental data are only available from the balance measurement. Note, the scale has been enlarged to reveal the details. UMARC/S predicts the vertical loads fairly well at most airspeeds. KTRAN and RDYNE over-predict the vertical loads.

Discussion/Future Work

The experimental data reported here have been dynamically corrected for the RTA/stand dynamic response. The Frequency Response Function (FRF) data used in determining the balance and shaft gauge dynamic calibration matrices and the non-rotating pushrod/balance response matrix were all obtained at a zero degree shaft angle. Reference 6 has shown that the RTA/stand dynamics changes with the stand angle of attack. The airspeed sweep was taken over a relatively small angle of attack range (1° aft to 4.6° forward), hence the FRF/angle of attack corrections are neglected. Reference 6 showed that rotor speed and thrust preload had some influence on the RTA/stand FRFs for frequencies above 20-30 Hz. The influence of the various parameters (hub mass, shaft rotation, and thrust preload) on experimentally measured hub loads needs to be further investigated. Besides comparing the 5/rev hub load magnitudes, the phase angle for each hub load should also be compared.

Conclusions

A comparison of measured and predicted 5/rev hub loadings was presented for the Sikorsky S-76 5-bladed proof-of-concept BMR for an airspeed sweep from 40 to 150 knots at constant thrust. The measured hub loads were obtained from a fixed-frame balance, rotating shaft bending gauges, and rotating hub-mounted accelerometers. Hub load predictions were obtained from the Sikorsky KTRAN and RDYNE rotor codes, and the Sikorsky version of the UMARC analysis. All three analyses showed reasonably good correlation with the measured data. For all three analyses, it is necessary to include free wake modeling to capture the 5/rev hub loads.

UMARC/S captures the trend of hub loads versus speed, but tends to over-predict the loads at 40 knots. KTRAN predicts the 5/rev magnitudes very well at the mid-speed (60-140 knots), but does not predict the sharp increase at 150 knots. RDYNE shows different trends with the data at low airspeeds.

The influence of the dynamic corrections on the balance and shaft gauge measurements was shown to be large for the 5/rev hub loads. The correction of the balance loading for the loading through the secondary load path was shown to be important for the pitch and roll moments. Good agreement was seen between the 5/rev drag force and pitch moments obtained from the balance and the shaft gauges. The shaft gauges show larger side force above 80 knots. Excellent agreement is seen in the roll moment measurements from 60 to 120 knots; the shaft gauge data show larger roll moments than the balance data below 60 knots and above 140 knots.

Acknowledgements

The authors wish to acknowledge the contribution of Randall Peterson, NASA Ames, in analyzing the shake test data, and helps from Kurt Hilzinger, Tim Krauss, Shyi-Yaung Chen, and Mike Torok of Sikorsky Aircraft in preparing the analytical calculations.

REFERENCES

1. Norman, T. R., Cooper, C. R., Fredrickson, C. A., and Herter, J. R., "Full-Scale Wind Tunnel Evaluation of the Sikorsky Five-Bladed Bearingless Main Rotor," Proceedings of the 49th Annual Forum of the American Helicopter Society, St Louis, MO, May 1993.

2. Wang, J. M., Duh, J., Fuh, J-S., and Kottapalli, S., "Stability of the Sikorsky S-76 Bearingless Main Rotor," Proceedings of the 49th Annual Forum of the American Helicopter Society, St Louis, MO, May 1993.

3. Wang, J. M., and Norman, T. R., "Correlation of Flatwise and Chordwise Bending Moments for a Sikorsky Full-Scale Bearingless Main Rotor," Proceedings of the AHS Aeromechanics Specialists Conference, San Francisco, CA, Jan 1994.

4. Sopher, R., and Chen S. Y., "Application of Component Mode Synthesis to Modeling the Dynamic Response of Bearingless Main Rotors," Proceedings of the 48th Annual Forum of the American Helicopter Society, Washington D.C., June 1992.

5. Gabel, R., Sheffler, M., Tarzanin, F., and Hodder, D., "Wind Tunnel Modeling of Rotor Vibratory. Loads," Proceedings of the 38th Annual Forum of the American Helicopter Society, Anaheim, CA, May 1982.

6. van Aken, Johannes, Peterson, R. L., and Freedman, C. J., "Calibration Results of the NASA Ames Rotor Test apparatus Steady/Dynamic Rotor Balance," Proceedings of the AHS Aeromechanics Specialists Conference, San Francisco, CA, Jan 1994.

7. Egolf, T. A., "Helicopter Free Wake Prediction of Complex Wake Structures Under Blade-Vortex Interaction Operating Conditions," Proceedings of the 44th Annual Forum of the American Helicopter Society, Washington D.C., June 16-18, 1988.

8. Chopra, I., "University of Maryland Advanced Rotor Code: UMARC," Proceedings of the AHS Aeromechanics Specialists Conference, San Francisco, CA, Jan 1994.

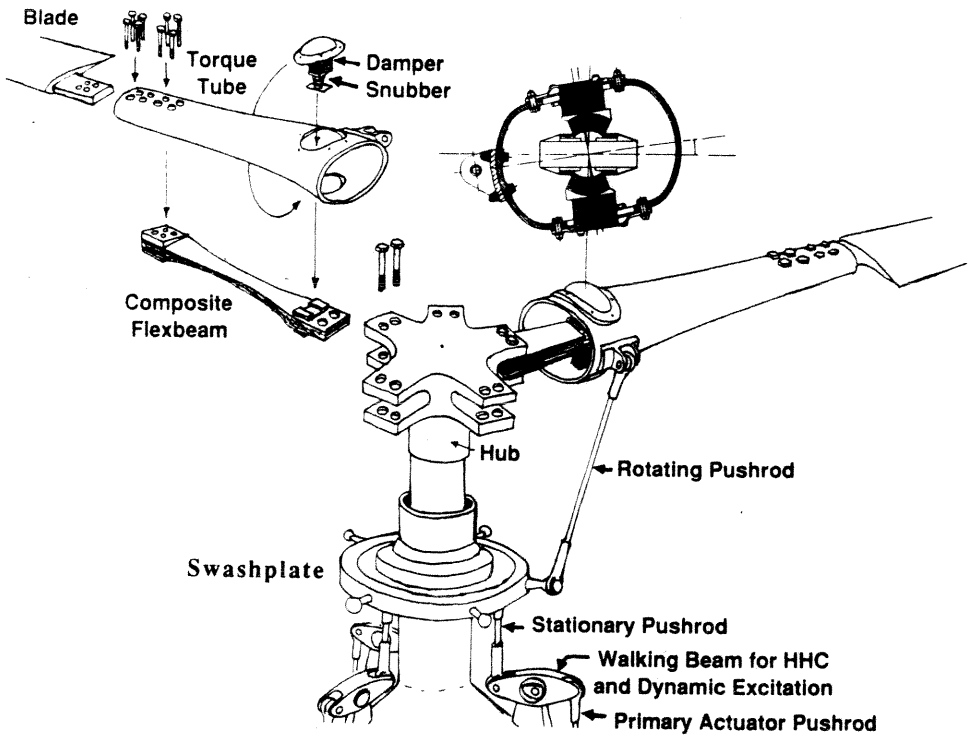

Figure 1 Sikorsky proof-of-concept 5-bladed BMR sized for the S-76 helicopter.

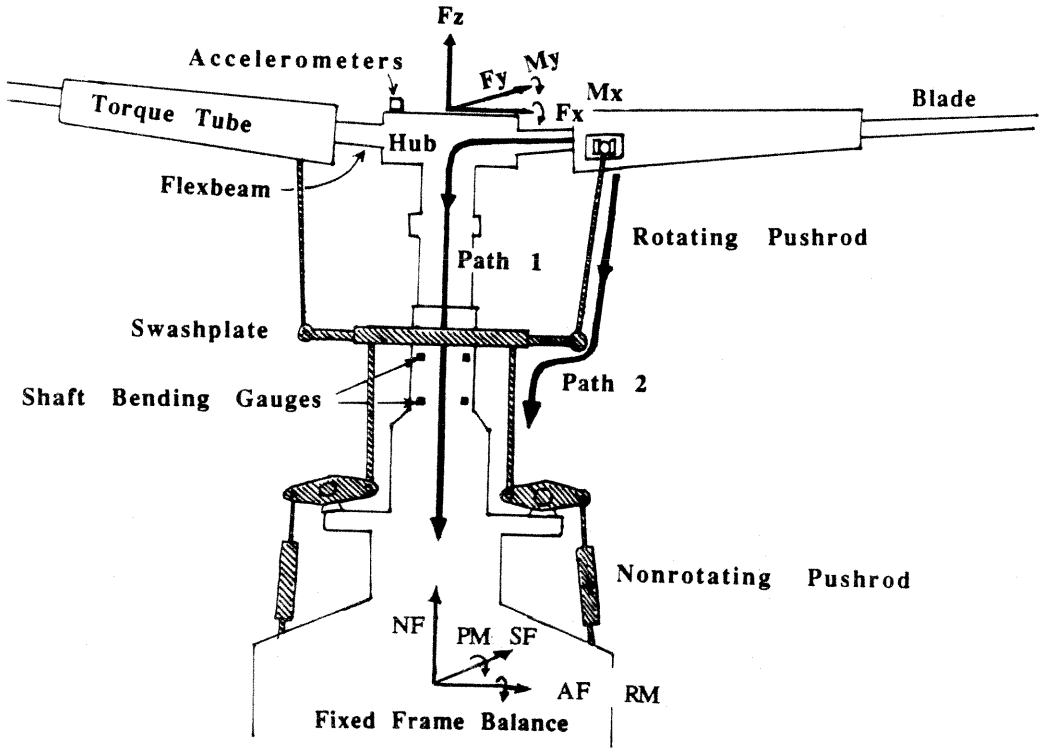

Figure 2 The redundant load path system. Also shown, the location of the rotating frame accelerometers and shaft bending gauges, and fixed frame balance for measuring vibratory hub loads.

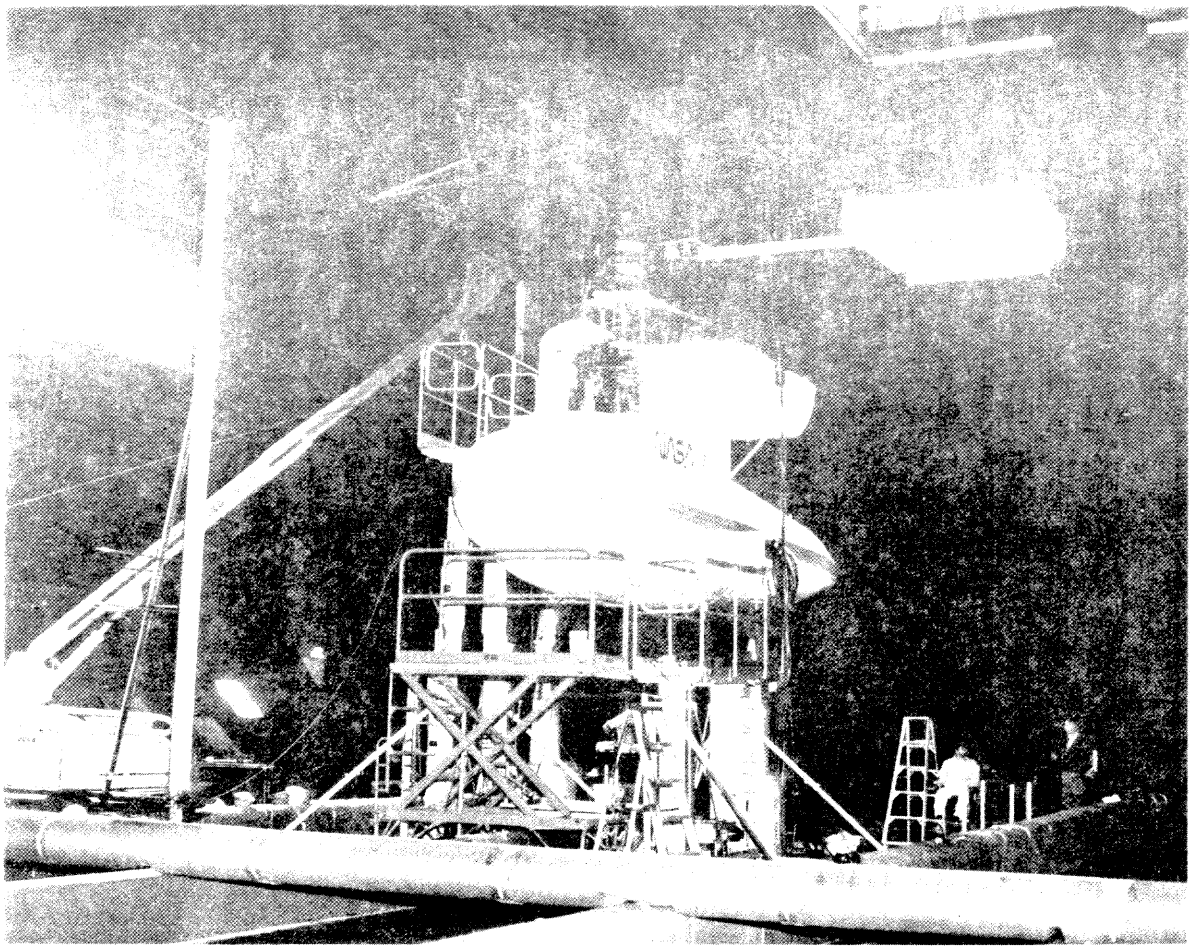

Figure 3 In the NASA Ames 40- by 80- Foot Wind Tunnel. Shake test setup for dynamic calibration of the RTA balance, shaft bending gauges, and hub accelerometers.

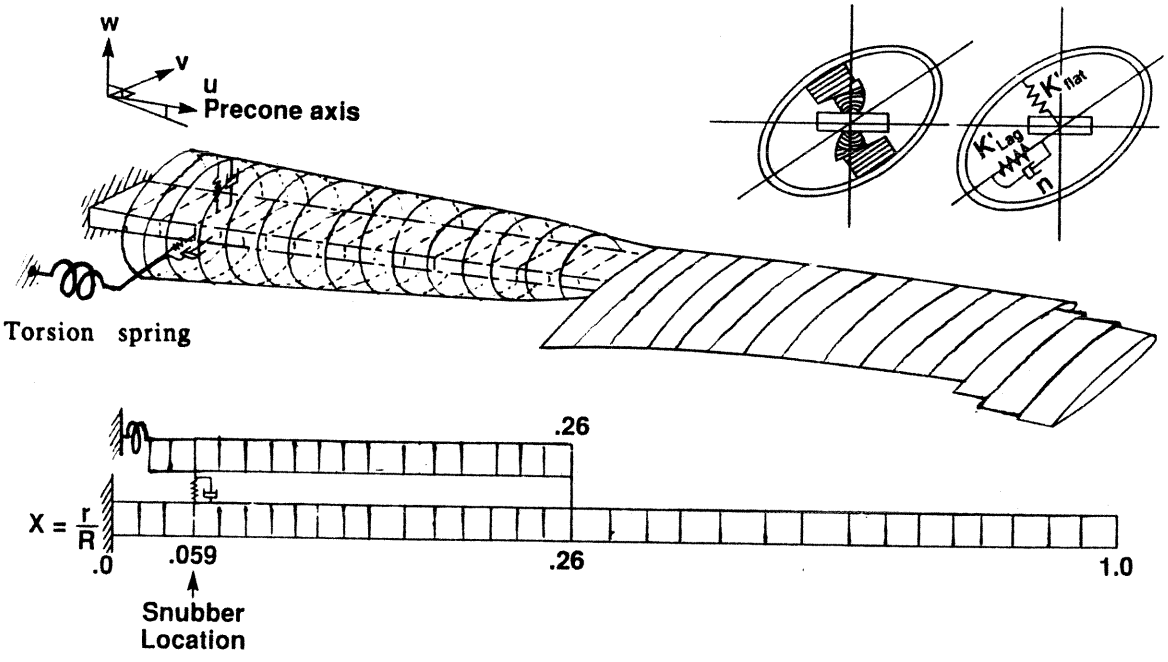

Figure 4 BMR model used in the Sikorsky KTRAN analysis.

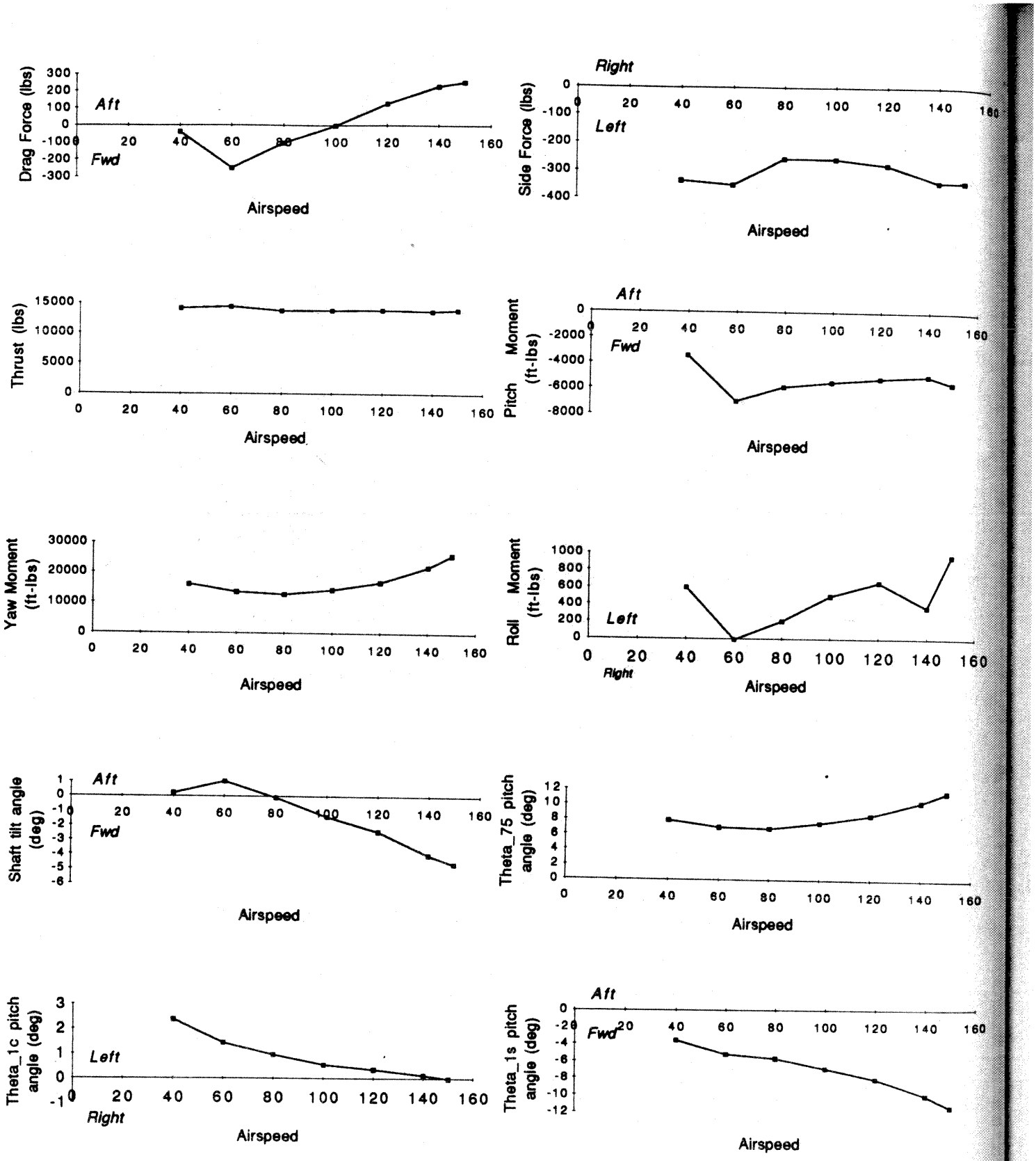

Figure 5 The steady trim values measured during the 40-150 knots airspeed sweep.

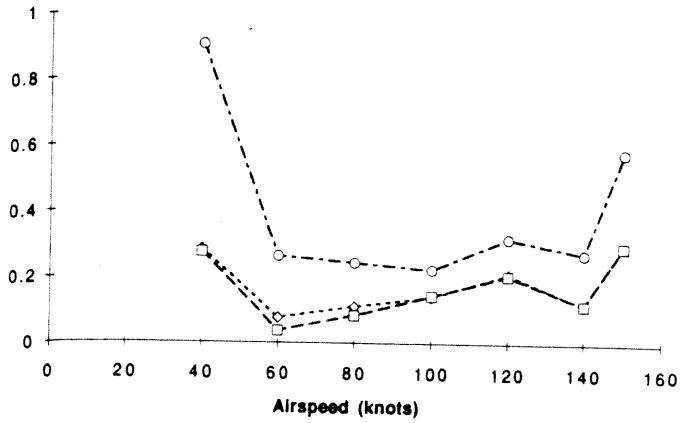

Figure 6a Drag force

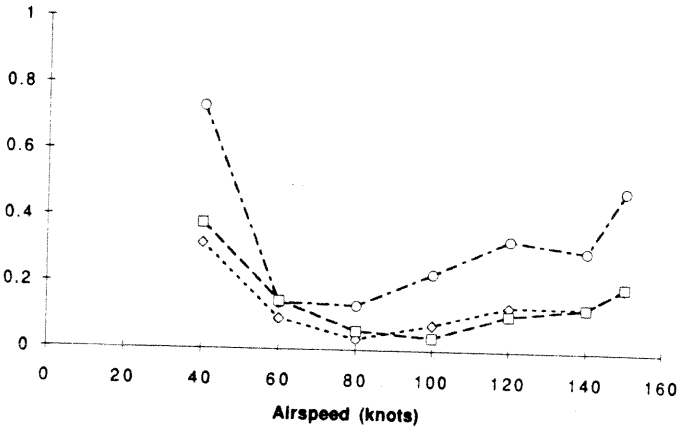

Figure 6b Side force

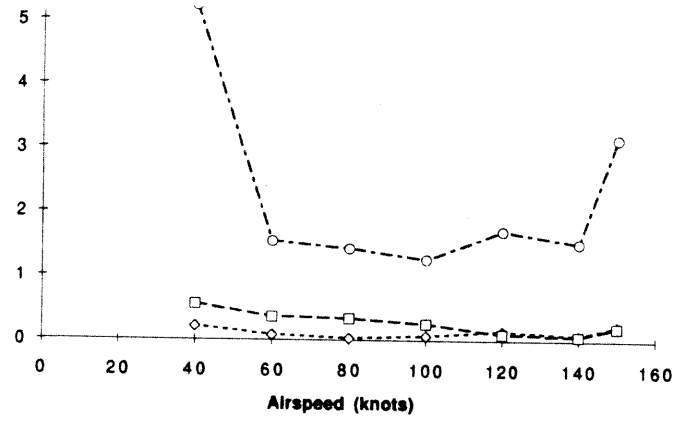

Figure 6c Pitch moment

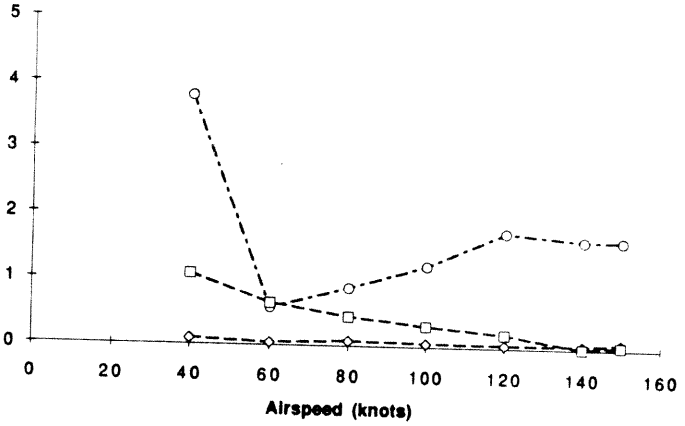

Figure 6d Roll moment

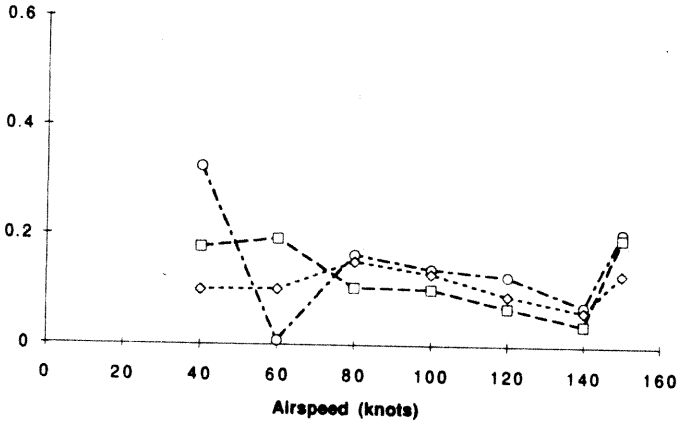

Figure 6e Vertical force

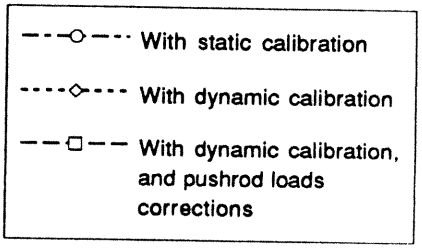

Figure 6 Normalized 5/rev vibratory hub loads measured by the rotor balance.

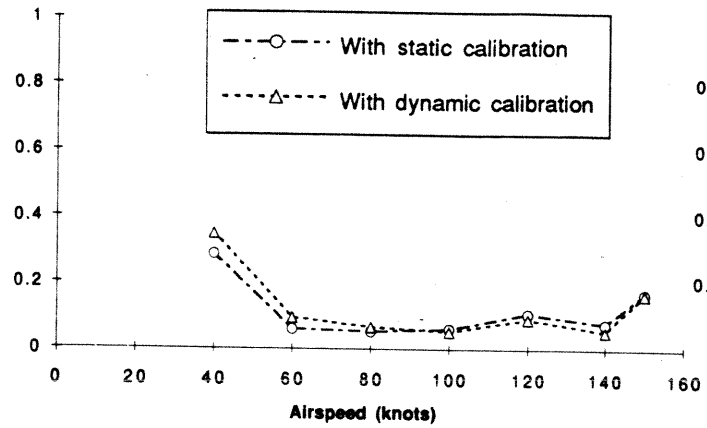

Figure 7a Drag force

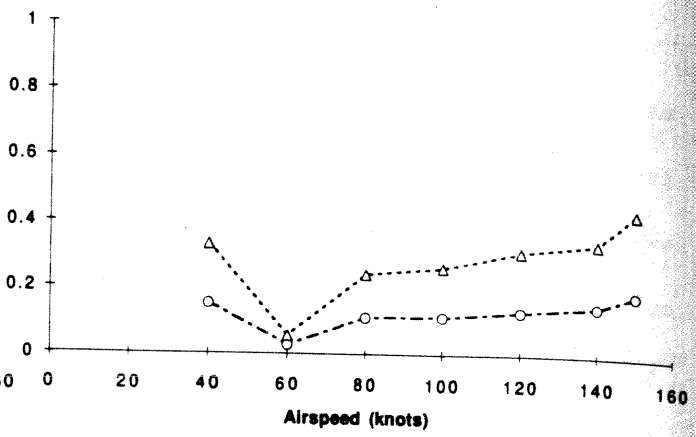

Figure 7b Side force

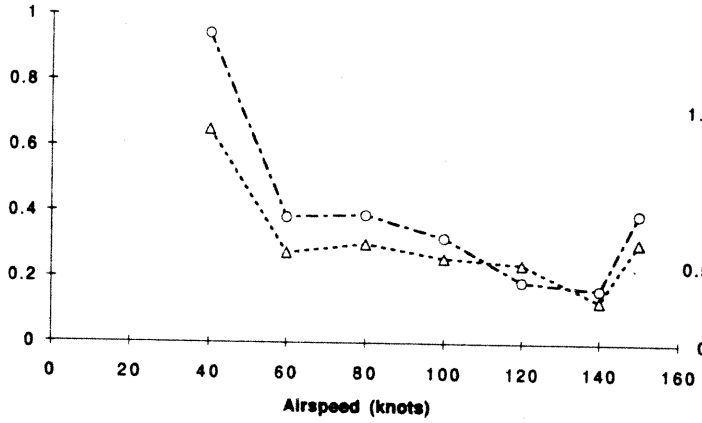

Figure 7c Pitch moment

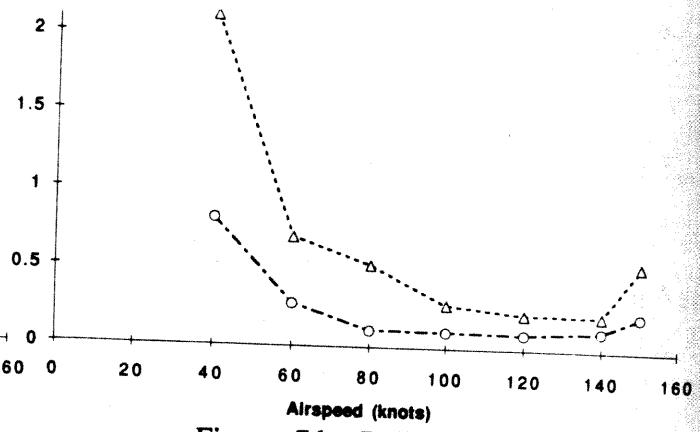

Figure 7d Roll moment

Figure 7 Normalized 5/rev vibratory hub loads measured by the shaft bending gauges.

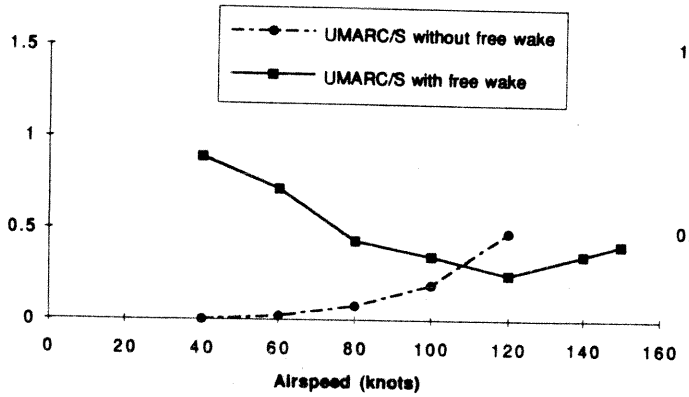

Figure 8a Pitch moment

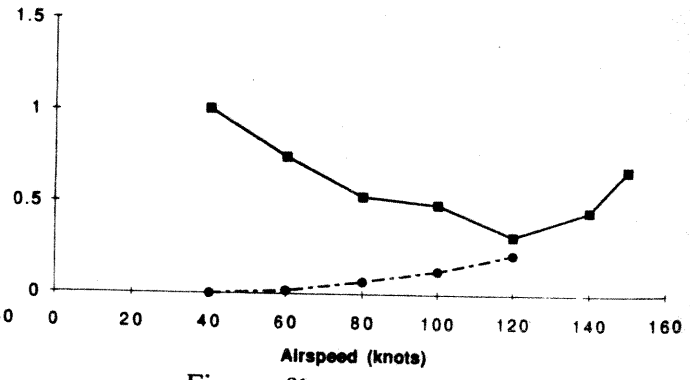

Figure 8b Roll moment

Figure 8 Normalized 5/rev pitch and roll moments predicted by UMARC/S.

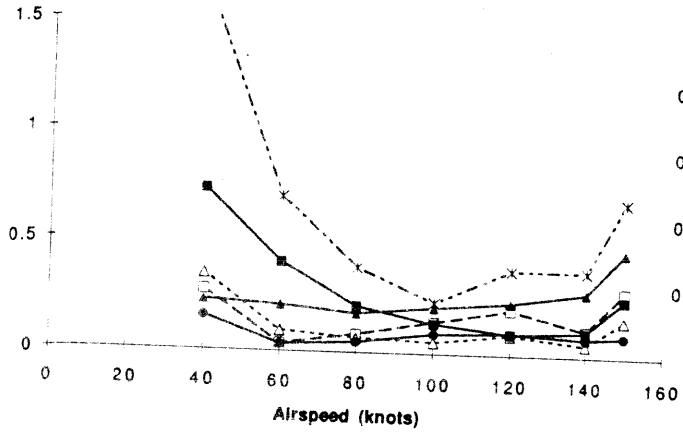

Figure 9a Drag force

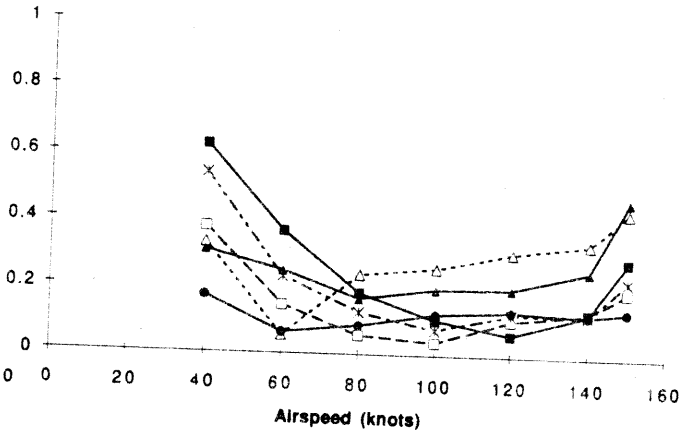

Figure 9b Side force

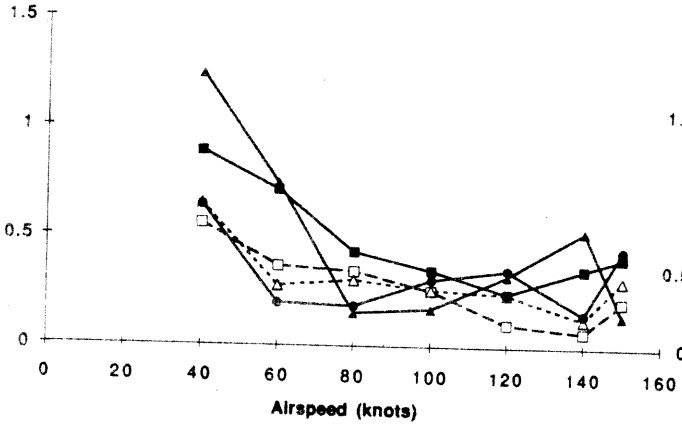

Figure 9c Pitch moment

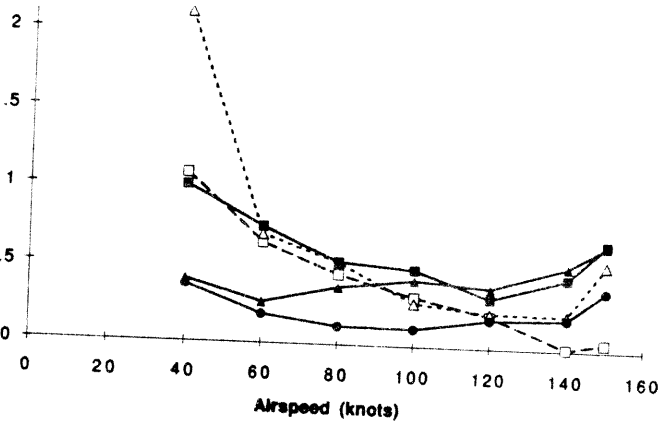

Figure 9d Roll moment

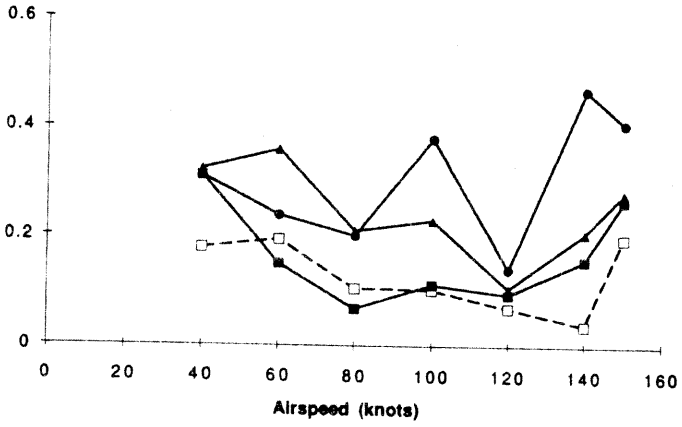

Figure 9e Vertical force

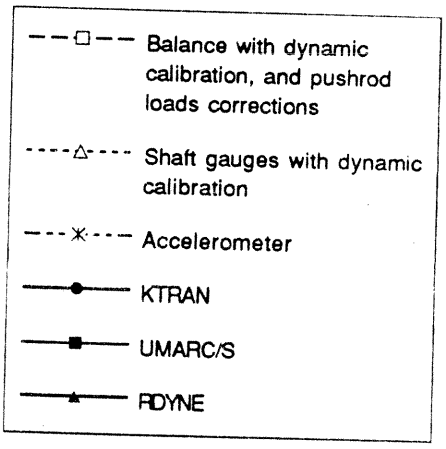

Figure 9 Comparison of measured and predicted normalized 5/rev vibratory hub loads.